iScience

CellPress
OPEN ACCESS

Article

Systematic analysis reveals a pan-cancer SNHG family signature predicting prognosis and immunotherapy response

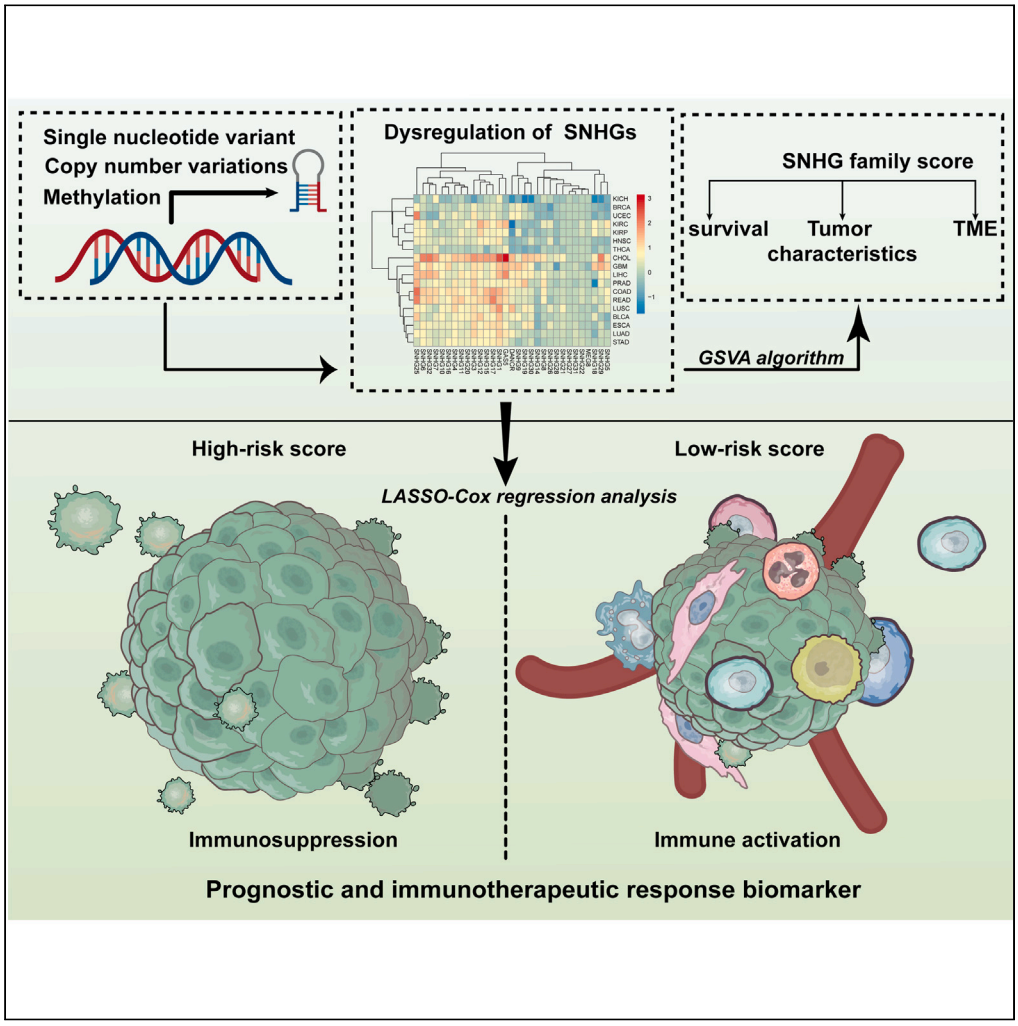

Haotian Zheng, Guanghui Wang, Yadong Wang, Jichang Liu, Guoyuan Ma, Jiajun Du

dujiajun@sdu.edu.cn

Highlights

Multi-omics analysis was performed to investigate the role of SNHGs in pan-cancer

SNHGs were biomarkers for prognosis and immunotherapeutic response

A pan-cancer signature of immunotherapeutic response was constructed

Zheng et al., iScience 26, 108055
October 20, 2023
https://doi.org/10.1016/j.isci.2023.108055

iScience

CellPress
OPEN ACCESS

Article

Systematic analysis reveals a pan-cancer SNHG family signature predicting prognosis and immunotherapy response

Haotian Zheng,[1,4] Guanghui Wang,[2,4] Yadong Wang,[1] Jichang Liu,[1] Guoyuan Ma,[2] and Jiajun Du[1,3,5,*]

SUMMARY

Small nucleolar RNA host genes (SNHGs) are a special family of long non-coding RNAs (lncRNAs), which not only function in a way similar to other lncRNAs but also influence the intracellular level of small nucleolar RNAs to modulate cancers. However, the features of SNHGs and their role in the prognosis and immunotherapeutic response of human cancer have not been explored. We found that SNHGs were commonly deregulated and correlated with patient survival in various cancers. The critical role of DNA methylation and somatic alterations on deregulation was also identified. SNHG family score was significantly associated with survival, multiple tumor characteristics, and tumor microenvironment. SNHG-related risk score could serve as a prognostic and immunotherapeutic response biomarker based on multiple databases. This study emphasizes the potential of SNHGs as biomarkers for prognosis and immunotherapeutic response, enabling further research into the immune regulatory mechanism and therapeutic potentials of SNHGs in cancer.

INTRODUCTION

Cancer immunotherapy (CIT) has emerged in recent years as a powerful weapon in fighting various cancers, depending on the interactions between the immune system and cancer.[1,2] Broad applicability across cancer types and durable clinical response extended overall survival (OS) relative to that achieved with conventional therapies.[3] Immune checkpoint inhibitors (ICIs) have achieved breakthroughs in multiple cancers, such as advanced melanoma (31–44% of patients' responses),[4–8] non-small cell lung cancer (19–20%),[9–11] and renal cell carcinoma (22–25%).[12,13]

However, CIT is not effective against all cancer types, particularly those with low tumor mutational burden (TMB).[1,14] The intricacy and uncertainty of tumor microenvironment (TME)—including T cell exhaustion and phenotype change, immune suppressive cell populations (regulatory T cell, myeloid-derived suppressor cell, type II macrophages), and cytokine and metabolite release (CSF-1, tryptophan metabolites, TGFβ, adenosine)[15]—cause immunotherapy to be ineffective for every patient within a "responsive" cancer type. Therefore, biomarkers need to be urgently developed to guide the selection of patients for immunotherapy or combination therapy, based on a full understanding of the basic biology of immunity.

Long non-coding RNAs (lncRNAs), defined as RNAs longer than 200 nucleotides that do not encode proteins, are involved in the pathogenesis of various cancers.[16] RNA–protein, RNA–RNA, or RNA–DNA interactions implemented by lncRNAs provide a new perspective into the regulatory mechanism in diverse biological characteristics of tumors (such as energy metabolism, drug chemoresistance, and immune regulation).[17–19] The innate and adaptive immune systems are extensively regulated by lncRNAs: the regulation of myeloid and dendritic cell development and functions; the regulation of immune genes and cytokine genes; and the differentiation of naive T helper cells into specialized effector populations of effector cells, and so on.[17,20–23] These findings contribute to the precision and effectiveness of cancer immunotherapies for multiple tumors to avoid immunotherapy resistance and improve efficacy.[24–26]

The small nucleolar RNA host genes (SNHGs) are a special group of lncRNAs. They perform their function in the nucleus (epigenetic modulation and transcriptional regulation) and cytoplasm (translation regulation, miRNA sponging, and posttranscriptional modification), similar to other lncRNAs,[27,28] as well as influence small nucleolar RNAs (snoRNAs) at the intracellular level; in addition, they play a growing role in cancer progression.[29,30] SNHGs play an important role in the TME and immune landscape, providing a theoretical basis for the development of immunotherapy.[31–34]

[1]Institute of Oncology, Shandong Provincial Hospital, Shandong University, Jinan, China
[2]Department of Thoracic Surgery, Shandong Provincial Hospital affiliated to Shandong First Medical University, Jinan, China
[3]Department of Thoracic Surgery, Shandong Provincial Hospital, Shandong University, Jinan, China
[4]These authors contributed equally
[5]Lead contact
*Correspondence: dujiajun@sdu.edu.cn
https://doi.org/10.1016/j.isci.2023.108055

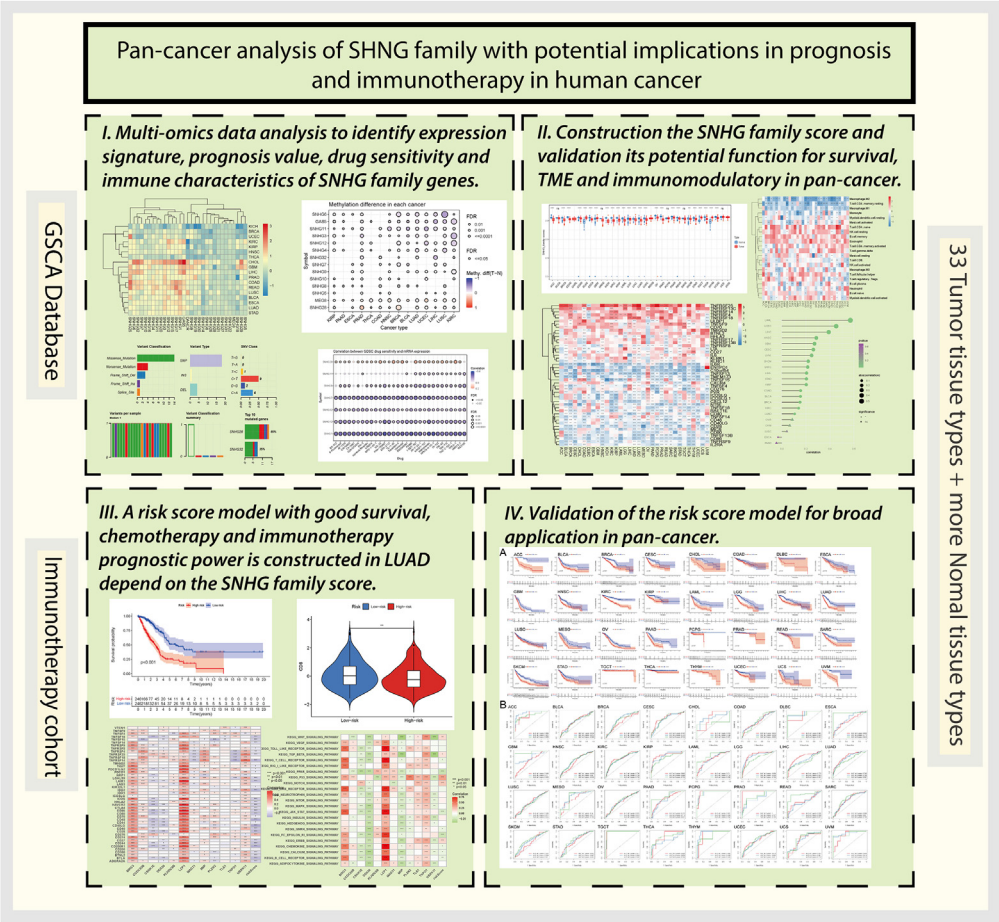

Figure 1. Analysis workflow of this study

In the current study, we report on a pan-cancer analysis of 31 SNHG genes across 33 cancers by using datasets from The Cancer Genome Atlas (TCGA), the Genotype-Tissue Expression (GTEx), and Gene Expression Omnibus (GEO). Pan-cancer analyses indicate that SNHG deregulation was affected by multiple mechanisms of mutation and methylation, which were associated with survival and drug sensitivity. The SNHG family score calculated based on the expression levels of SNHGs showed a significant difference between the normal and tumor samples. The association of the SNHG family score with patient survival and tumor progression in pan-cancer. Subsequently, the link between the SNHG family score and TME and immunotherapy was investigated. We further constructed the risk score by using 12 SNHG-related genes to clarify the functional role of the SNHG family score. We also explored the ability of the risk score to predict patient survival and tumor immunity. The association between risk score and tumor immunotherapy response was evaluated using four CIT response datasets and immunotherapy signatures. This study preliminarily unveiled the potential application of the SNHG-related risk score as a predictive biomarker of survival and immunotherapy response in pan-cancer; however, further research is still needed.

RESULTS

Basal expression and prognostic potential of SNHGs

The overall design of our study is shown in the flow chart (Figure 1). The distribution of the 24 SNHGs expression levels of patients for 33 cancers is presented in Figure 2A, and SNHGs with low expression level in pan-cancer were excluded. SNHGs exhibited significant differential expression in most cancers (Figure 2B), suggesting that the SNHGs played a distinctive role in tumorigenesis. SNHG19 was significantly lower expressed in KICH, but GAS5 was significantly higher expressed in CHOL, which suggested that SNHGs could be used as a potential biomarker in cancers. Differences in OS, disease-specific survival (DSS), disease-free interval (DFI), and progression-free survival (PFS) between high- and low-gene expression groups were measured to investigate the prognostic potential of SNHGs in human cancers (Figure 2C). Univariate Cox regression analysis based on SNHGs showed that most SNHGs were associated with survival time in pan-cancer, particularly with OS and PFS. Meanwhile, SNHGs had more significant predictive potential for KIRC and ACC.

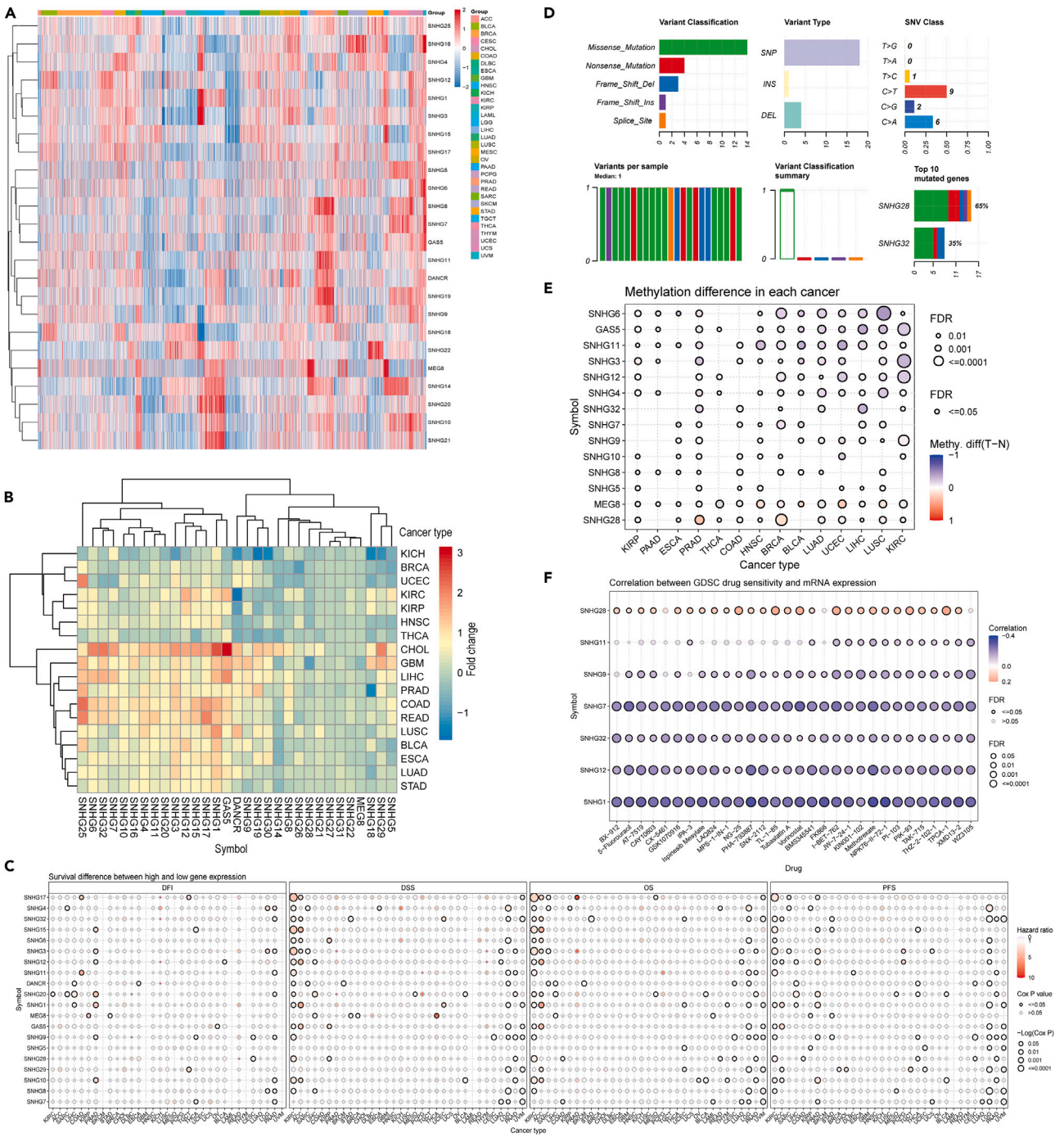

Figure 2. Expression, mutations, methylation and drug sensitivity landscape of small nucleolar RNA host genes in human cancer

(A) Heatmap showing the expression levels of SNHGs among all samples grouped by cancer.

(B) Significant difference of expression level of SNHGs between normal and tumor samples in 15 cancer types. FDR are shown along the right.

(C) Univariate Cox regression analysis of OS, DSS, DFI and PFS of low and high groups stratified by the expression levels of SNHGs in Pan-cancer. Somatic mutations alteration (D), differential methylation (E) and drug sensitivity (F) of SNHGs were performed in human cancers.

SNHG deregulation affected by mutations and methylation and is associated with drug sensitivity

To elucidate the mechanism underlying the effect of SNHGs on tumorigenesis, we further investigated the DNA methylation, somatic mutations, and copy number alterations of SNHGs in human cancers. The results for the somatic mutations are shown in Figure 2D. SNHG28 (65%),

and SNHG32 (35%) were the most frequently mutated SNHGs. SNHG28 mutation occurred mainly in UCEC, CESC, READ, and BRCA (Figure S1A). The CNVs of SNHGs were mainly found in UCS, LUAD, KICH, and CHOL (Figure S1C). THCA and LAML showed few alterations in CNVs (Figure S1C). Most CNAs were amplifications. SNHG amplifications were enriched in SNHG17, SNG11, SNHG15, and SNHG6. Copy number amplification was positively related with SNHG expression in pan-cancer (Figure S1B). SNHGs were generally hypomethylated in 14 cancers (Figure 2E). However, MEG8 and SNHG28 were hypermethylated in most cancers. DNA methylation changed consistently with high SNHG expression (Figures 2B, and S1D). Meanwhile, differential methylation was related to OS, DSS, DFI, and PFS (Figure S1E).

On the basis of the importance of SNHG in tumor progression, we analyzed the correlation between SNHG and chemosensitivity. SNHG1, SNHG12, SNHG32, and SNHG7 each exhibited a significant negative correlation with sensitivity to various chemotherapeutic agents (Figure 2F). However, patients with high SNHG28 expression exhibited better drug sensitivity (Figure 2F). Combining the aforementioned results, we find that SNHG28 was a distinctive SNHG with high methylation, low expression, high mutation, and positive drug sensitivity.

SNHG family score differentially expressed and significantly associated with survival in pan-cancer

For revealing the expression patterns of SNHG family genes, we calculated the SNHG family score of 33 tumor and normal tissues, based on the gene expression data from TCGA and GTEx. All cancers presented a high SNHG family score, indicating that the lncRNA family had high expression levels in various cancers (Figure 3A). Excluding 3 cancers with inadequate normal tissue samples (CHOL, MESO, UVM), we compared the SNHG family score between the tumor and normal tissues. The results showed that 25 of these 30 cancers had significantly different expressions of SNHG family scores (Figure 3A). Most cancers had lower SNHG family scores, compared with the normal samples; meanwhile, DLBC, GSM, TGCT, and THYM showed higher scores compared with the normal samples (Figure 3A).

KM curves indicated that the high SNHG family score was related to the poor OS rates in ACC, LIHC, HNSC, SARC, KICH, KIRC, and DLBC but related to the high OS of ESCA, GBM, OV, BLCA, LUAD, LUSC, CESC, UVM, STAD, and PAAD (Figure S2).

Role of SNHG family score in tumor microenvironment and immunotherapy response of human cancers

Functional relevance analysis showed that the SNHG family score was correlated with 14 biological functions in pan-cancer (Figure 3B). EMT, metastasis, and invasion were more correlated with the SNHG family score than the indicator of tumor cell growth (cell cycle, proliferation). Hypoxia, inflammation, and angiogenesis, which can significantly affect the tumor immune environment, were highly correlated with the SNHG family score. This conclusion was more evident in LUAD. Accordingly, we investigated the correlation between the TME score and the SNHG family score. The SNHG family scores were negatively related to the immune score in 14 cancers; by contrast, an opposite relationship with the immune score was observed in THYM (Figure 3C). Given the importance of stromal cells as mediators of immune function and response to immunotherapies,[35] we analyzed the stroma score on the basis of the xcell algorithm. The stroma score was positively related to the SNHG family score in LAML, UCEC, LGG, THCA, and CESC. The opposite result was observed in 8 cancers (TGCT, COAD, UCS, LIHC, STAD, LUAD, LUSC, and KIRC), consistent with the finding that stromal cells played a heterogeneous role in pan-cancer.[36] We further performed detailed correlation analyses between immune cells and the SNHG family score in human cancers. The SNHG family score exhibited a higher similarity in the correlation with immune cells in pan-cancer (Figure 3E). The M2 macrophage was negatively related to the SNHG family score in 25 cancers, and the $CD4^+$ memory resting T cell and the macrophage M1 were correlated with the SNHG family score (Figure 3E). The expression levels of immune-activating (Figure S3A) and suppressing genes (Figure S3B), chemokine (Figure S3C), and chemokine receptor (Figure S3D) genes were correlated with the SNHG family score. These results show that the SNHG family score can be a key factor influencing the immune environment.

Based on the functional and immune analyses, we analyzed the immunotherapy predictive value of SNHG family score**.** The correlation of the SNHG family score with TMB, MSI, and TIDE scores was determined to evaluate the potential immunotherapeutic response. The results indicated that the SNHG family score was associated with TMB in 17 cancers (Figure 3F). Further, 6 of the cancers (LAML, THCA, KIRC, COAD, BRCA, VCEC) were positively associated. The MSI of 18 cancers were positively related to the SNHG family score, whereas THYM was negatively related (Figure 3G). According to the TIDE score of 22 cancers, higher SNHG represented higher TIDE score in 17 pan-cancer (Figure 3I). The SNHG family score was associated with immune checkpoint expression in diverse cancer types, particularly with PD-L1 (Figure 3H). The correlation analysis between the SNHG family score, combined with immunotherapy markers and immune checkpoints, indicates that the SNHG family score can be a negative predictor of immunotherapy response in pan-cancer.

Construction of SNHGs related risk score in LUAD

The aforementioned data indicate that the SNHG family score plays significant functional roles in pan-cancer, particularly in LUAD. Accordingly, in this study, we aimed to further clarify the functional role of the SNHG family score in LUAD. LUAD patients were divided into high and low SNHG family scores, and patients in the low-score group had significantly poorer clinical outcomes than those in the high-score group (Figure 4A). The results of the differential analysis between the two groups revealed 2566 genes (Figure 4B). Combined with the GEO validation cohort, 2179 intersection genes were screened. Univariate cox regression analysis further screened out 387 prognostic differential genes associated with the SNHG score. A prognostic model consisting of 12 genes (BIRC3, CCDC85B, CSNK1E, DDX56, KLHDC8B, LCP1, MAGT1, MIIP, PLEK2, TLE1, TNPO1, and UBXN11) was established by LASSO–Cox regression analysis (Figures S4A, and S4B). The risk score was calculated accordingly. The calculation formula and regression coefficient are listed in Table S3. The LUAD patients were stratified into either high-risk (n = 246) or low-risk group (n = 246), depending on the median cutoff of the risk score in the TCGA-LUAD cohort.

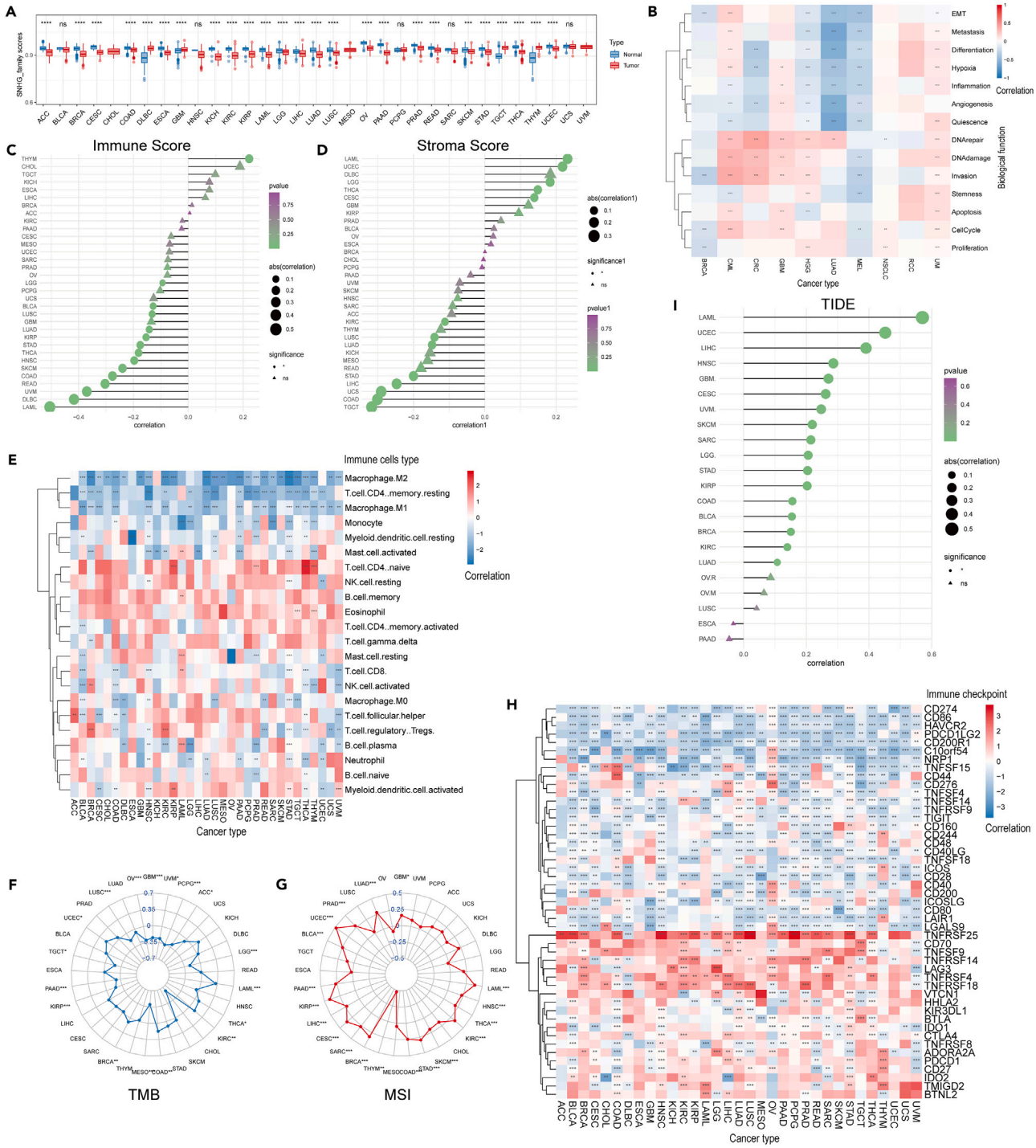

Figure 3. Role of SNHG family score in Functional relevance analysis, tumor microenvironment and immunotherapy response of human cancers

(A) Significant difference of SNHG family score between normal and tumor samples in 33 cancer types.

(B) The correlation between the SNHG family score and the 14 functional states of pan-cancer at a single-cell resolution by CancerSEA. The correlation between the SNHG family score and immune score (C), stroma score (D) and 22 immune cells (E). The correlation between the SNHG family score and TMB (F) and MSI (G), the location of the dot represents the correlation coefficient. (H) Heatmap showing the correlation between the SNHG family score and the expression level of immune checkpoints. (I) The correlation between TIDE scores of 22 cancers and SNHG family score. *p < 0.05; **p < 0.01 and ***p < 0.001, ****p < 0.0001; ns, not significant.

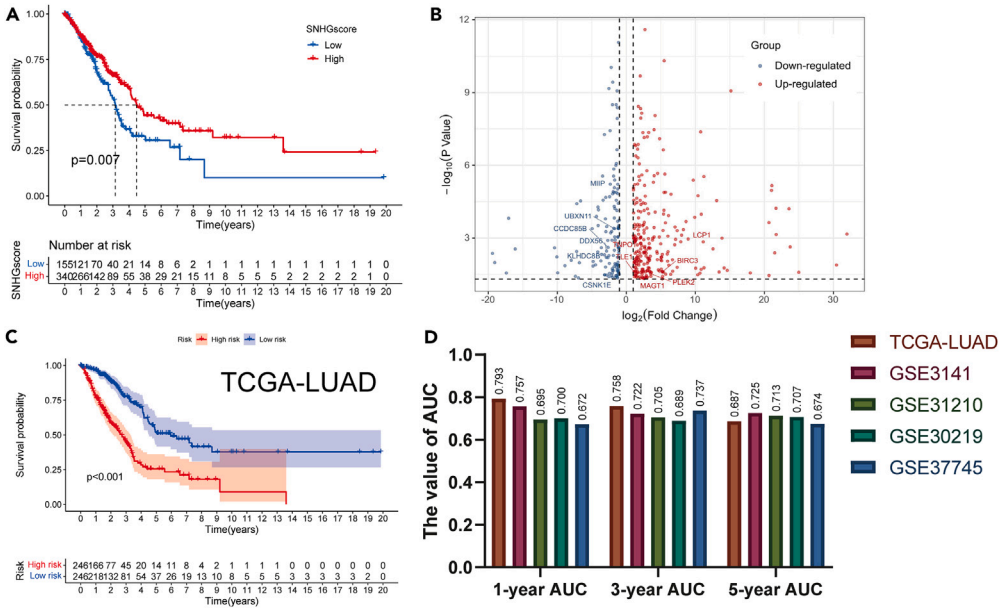

Figure 4. SNHGs related risk score in LUAD

(A) Kaplan–Meier curves of low and high groups stratified by the SNHG family score in LUAD.

(B) Differential analysis between low- and high-SNHG family score groups in LUAD.

(C) KM survival analysis of SNHG-related risk score in TCGA cohort.

(D) The AUC of SNHG-related risk score were performed in TCGA cohort and 4 GEO validation cohorts: GSE3141; GSE31210; GSE30219 and GSE37745.

SNHG-related risk score as a significant prognostic factor in LUAD and other cancers

KM survival analysis ($p < 0.001$, Figure 4C) and ROC (1-, 3-, and 5-year AUC = 0.793, 0.758, 0.687, Figure 4D) indicated the good survival predictive ability of the risk score, which finding was verified by the GEO validation cohorts (Figures 4D; and S4E): GSE3141 (KM survival analysis $p = 0.007$; 1-, 3-, and 5-year AUC = 0.757, 0.722, 0.725); GSE31210 (KM survival analysis $p = 0.011$; 1-, 3-, and 5-year AUC = 0.695, 0.705, 0.713); GSE30219 (KM survival analysis $p = 0.001$; 1-, 3-, and 5-year AUC = 0.7, 0.689, 0.707); and GSE37745 (KM survival analysis $p < 0.001$; 1-, 3-, and 5-year AUC = 0.672, 0.737, 0.674). The results of the risk factor analysis showed a correlation between the risk score and the survival status in TCGA-LUAD and GEO validation cohorts (Figure S4F). Univariate and multivariate Cox regression analyses were conducted to analyze whether the risk score could be an independent prognostic factor in LUAD. The risk score and other clinical characteristics were used as covariates. The results indicated that the stage and risk score were significantly associated with OS in LUAD and could be considered independent prognostic factors (Figures S4C, and S4D). To further investigate the clinical potentiality of the risk score in LUAD, a correlation analysis between clinical characteristics and risk score was implemented. The results indicated that T, N, and the stage were significantly correlated with the risk score; by contrast, age, gender, and M were not (Figure S4G).

Meanwhile, we generalized the risk score for pan-cancer to evaluate the fitness of the model. KM survival analysis and ROC were used to evaluate the prognostic value of the risk score in other cancers (KICH was excluded because of raw data). In 30 types of cancer (excluding COAD and TGCT), patients in the high-risk group had significantly poorer clinical outcomes than those in the low-risk group ($p < 0.05$, Figure S5A; and Table S4). The ability to evaluate the sensitivity and specificity was in some cancers (ACC, DLBC, PCPG, UVM, etc. Figure S5B) than in LUAD.

SNHG-related risk score is a stronger predictor for immune signatures in LUAD

To explore the reasons for the significant effect of the risk score on the survival of cancer patients, we conducted functional studies of the risk score. We calculated pathway activity and hallmark scores for each patient by using the ssGSEA algorithm and measured the association between the risk score and these functional scores. The risk score was positively related to the hallmark scores of hypoxia and glycolysis, which were recently identified as critical factors for the development of cancer and immunotherapy[37–39] (Figure 5A). Moreover, multiple classical cancer-promoting pathways (WNT, P53, and NOTCH pathways, etc.) were positively correlated with the risk score (Figure S6A), further explaining the poorer survival of the high-risk group.

Using associations with master immune regulators (TGF-beta pathway, etc.) (Figure 5A), we explored the relationships between the risk score and tumor immunity. The stromal score, immune score, and ESTIMATE score were lower in the high-risk group (Figure 5B). The scores of immune cells and immune-related pathways via ssGSEA were also lower in the high-risk group (Figures 5C and 5D). On the basis of the MCP-counter, we analyzed the differential immune cells and stromal cells between the two groups. $CD8^+$ T/T cells, B cells, monocytes,

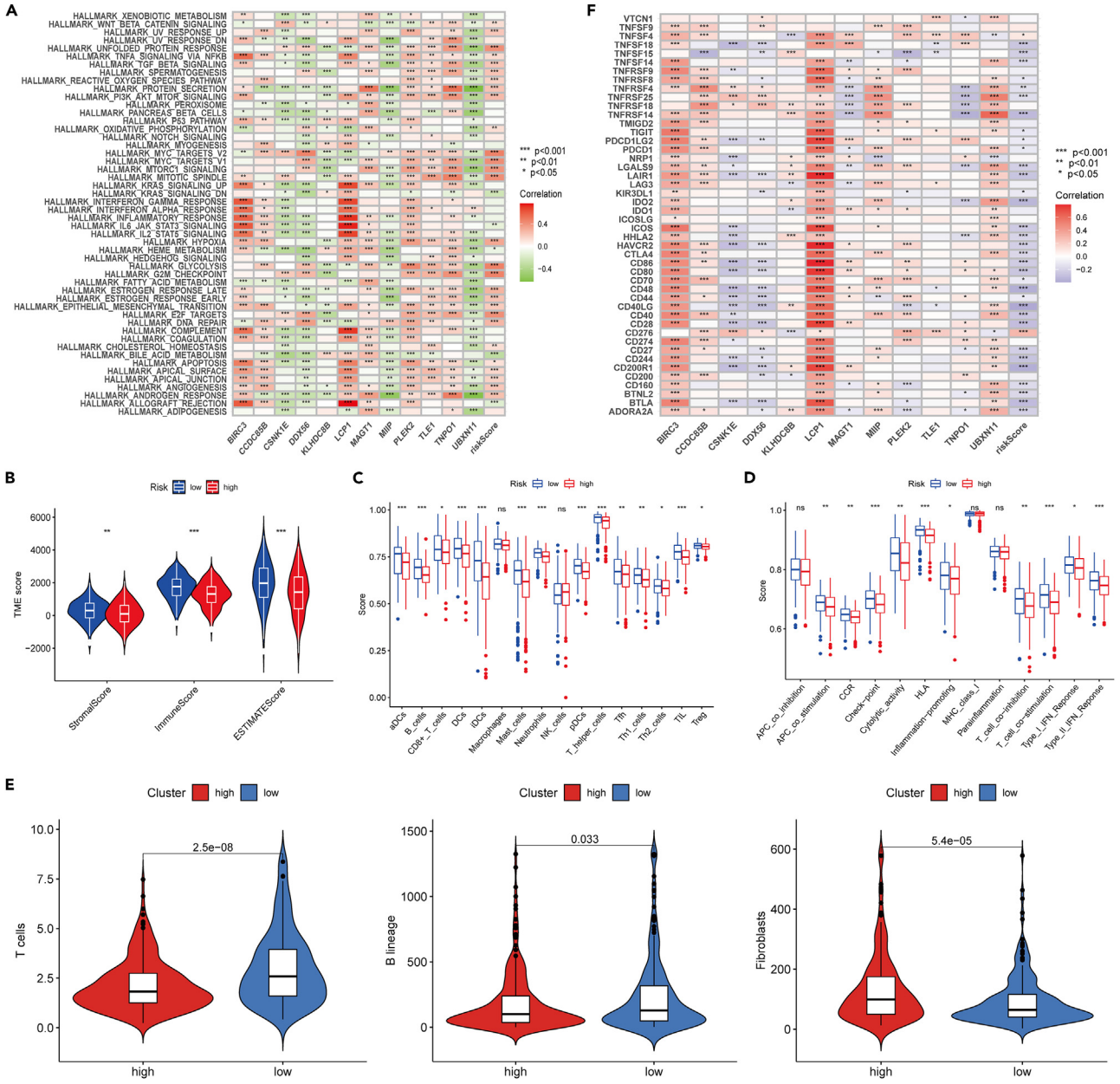

Figure 5. SNHG-related risk score is a stronger predictor for immune signatures in LUAD

(A) The correlation between SNHG-related risk score and hallmark pathway scores. Differential analysis between low- and high-SNHG-related risk score groups of TME score(B), the scores of immune cells (C) and immune-related pathways (D) by ssGSEA.

(E) Differential immune cells and stromal cells between low- and high-risk score groups based on MCP-counter.

(F) Heatmap showing the correlation between the risk score and the expression level of immune checkpoints.

and neutrophils were higher in the low-risk group than in the high-risk group (Figures 5E, and S6B). However, cancer-promoting fibroblasts were higher in the high-risk group than in the low-risk group (Figure 5E). These results suggest that the risk score may influence tumor immunity primarily by mediating immune cell activity.

SNHG-related risk score can potentially predict immunotherapy response in LUAD and other cancers

The aforementioned results and the observed negative associations between the risk score and the expression levels of immune checkpoint genes (Figure 5F) suggest that the risk score may correlate with the response to immunotherapy. To test this hypothesis, we investigated the correlation between the risk score and two immunotherapy predictors (TIDE and IPS) and four immunotherapy cohorts

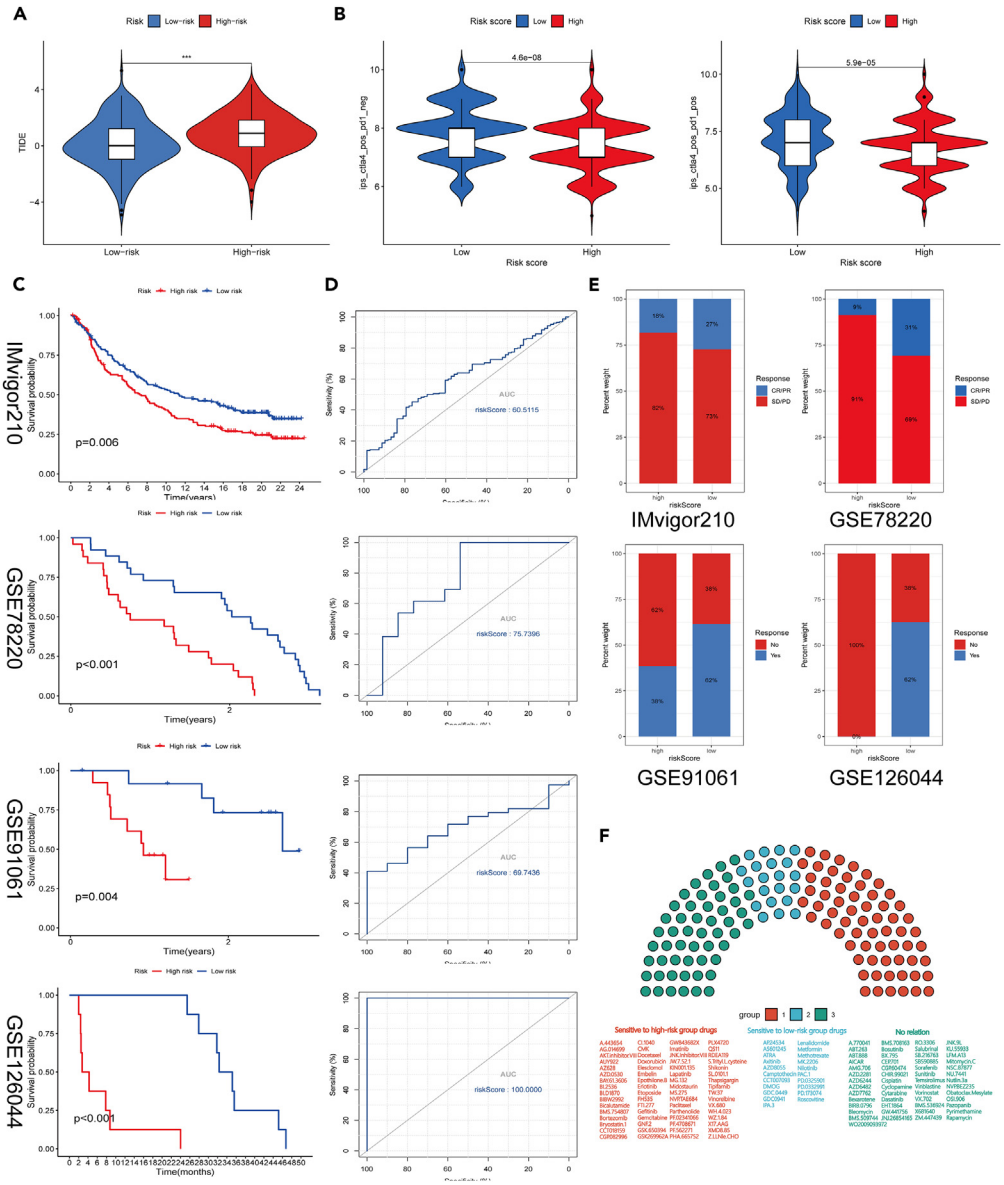

Figure 6. SNHG-related risk score can potentially predict immunotherapy response in LUAD and other cancers

(A) Difference of TIDE in low- and high-risk score.

(B) Difference of IPS with CTLA4+ and PD-1- and CTLA4+ and PD-1+ between low- and high-risk group. Survival analyses (C), ROC curves (D) and response to immunotherapy (E) of between low- and high-risk groups in 4 immunotherapy cohorts (IMvigor210, GSE78220, GSE91061, and GSE126044).

(F) Drug sensitivity analyses between low-and high-risk groups. Blue, sensitive to patients with low-risk scores; Red, sensitive to patients with high-risk scores; Green, no sense. *p < 0.05; **p < 0.01 and ***p < 0.001; ns, not significant.

(IMvigor210, GSE78220, GSE91061, and GSE126044). In TIDE, dysfunction, and exclusion scores, immunotherapy is still more suitable for the low-risk group than the high-risk group (Figures 6A, S6C, and S6D). Patients in the low-risk group were more sensitive to immunotherapy (the PD-1 inhibitor and combined PD-1 and CTLA4 inhibitors) as determined from the IPS analysis of the four modules (Figure 6B). We also used the IPS score to evaluate the predictive ability of the risk score in the other 19 pan-cancer immunotherapies (Table S5). The risk score was associated with the immunotherapy response in most cancers, particularly in combination immunotherapy. Meanwhile, in the immunotherapy cohorts, the prognosis of the high-score group was worse than that of the low-score group (Figure 6C). We found that the immunotherapy response rate was higher in the low-score groups than in the high-score group (Figure 6E). The ROC of the immunotherapy response rate showed that the risk score exhibited good sensitivity and specificity in immunotherapy prediction (Figure 6D). Notably, the data indicated that the risk score was associated with the immunotherapy response and could be a potential biomarker for immunotherapy response.

In addition, to provide patients with a more detailed treatment plan, we compared the sensitivity of the chemotherapy drugs between the high- and low-risk groups. Compared with the low-risk patients, the high-risk patients were more sensitive to 64 chemotherapy drugs (Figure 6F). However, 21 chemotherapy drugs were more suitable for low-risk than high-risk patients.

DISCUSSION

Growing evidence has suggested the association of SNHGs with tumor progression, prognosis, and treatment response.[31–34] Integrating the pan-cancer data, we systematically analyzed the expression dysregulation of the SNHG family between the normal and tumor samples and DNA methylation, genomic changes, prognostic potential, involved functional status, and correlation with tumor immunity and the immunotherapeutic response in pan-cancer. Results showed the expression landscape of these 31 SNHGs in 33 cancers. SNHG expression was lower in LIHC than in other cancers, and SNHG29 was the most abundantly expressed gene in all 33 cancers. A significant difference in SNHG expression was found between different types of cancer and normal tissues. Some cancers showed higher expression levels, whereas other cancer types exhibited lower expression levels, compared with the normal samples, such as SNHG5. The cancer-specific feature was consistent with existing reports.[40,41] Meanwhile, SNHGs were significantly correlated with patient survival in diverse cancers.

As key factors in cancer cell dysregulation,[42] DNA methylation and genomic changes can affect SNHG expression; thus, differential DNA methylation, SNVs, and CNVs were analyzed. Genomic changes were primarily observed in SNHG28 and SNHG32, mainly influencing UCEC, CESC, READ, and BRCA. CNVs dominated by amplification caused the aberrant upregulation of SNHGs, but pervasive hypomethylation induced the aberrant downregulation. These epigenomic and genomic changes may be responsible for the complicated and cancer-specific dysregulation of SNHGs in cancer. Meanwhile, the OS, DSS, DFI, and PFS of the patients were related to differential methylation. Further chemosensitivity analysis found that SNHGs were significantly correlated with sensitivity to various chemotherapeutic agents. Notably, we found a distinctive SNHG (SNHG28) with high methylation, low expression, high mutation rate, and positive drug sensitivity, in contrast to other SNHGs. However, almost no literature reviews related to SNHG28 have been reported. Thus, the role of SNHG28 in tumor development deserves further study.

With the role of SNHGs in tumorigenesis and tumor development considered, investigating their role in different types of cancer is crucial. The SNHG family score was calculated for the overall evaluation of the role of all SNHGs in pan-cancer. We comprehensively analyzed the SNHG family score of 30 cancers (3 other cancer types lack adequate normal tissues). A significant difference in the SNHG family score was found between the tumor and normal samples in 25 cancers, and most cancer samples had lower SNHG family scores, compared with the normal samples. Meanwhile, a low SNHG family score was related to poor OS, as indicated by the KM curves. These results indicate that the SNHG family score was a cancer-suppression biomarker in most cancer types.

To investigate the role of SNHGs in cancer progression, we analyzed their functions and pathways. The results indicated that SNHGs were associated with the TME. Inflammation, angiogenesis, and hypoxia are hallmarks of cancer that substantially contribute to the development and progression of malignancies by regulating TME and therapy resistance.[43–45] Hypoxia, inflammation, and angiogenesis at the single-cell level were related to the SNHG family score. This result provided an opportunity for targeting these SNHGs to improve patient outcomes. Considering the role of hallmarks in TME and the association between SNHG family-related genes and immunity in gliomas,[46] we analyzed the relationship between the SNHG family score with tumor immunity. The immune score, stromal score, and immune-related genes were significantly related to the SNHG family score. As the most abundant infiltrative immune cells present in and around tumors, macrophages have drawn research interest.[47] Macrophage populations can be polarized into the classically activated type, M1, which inhibits growth or kills, and M2, which produces ornithine, VEGF, EGF, and TGF–β to promote growth and repair.[48,49] The macrophage M2 was negatively related to the SNHG family score in 25 cancers, which was consistent with the cancer suppression feature in most cancer types.

Given that the SNHG family score is a critical regulator of TME and tumor immunity, we further systematically analyzed the correlation between the SNHG family score and immunotherapy. In the analysis, we considered diverse immunotherapy signatures, including TMB, MSI, TIDE, and immune checkpoint. We observed that the SNHG family score was highly correlated with these immunotherapy signatures. The target of PD-L1 immunotherapy was negatively associated with the SNHG family score. In combination with the analytical results of TMB and TIDE, the high SNHG family score may represent a low response rate to immunotherapy. However, MSI exhibited an inverse relationship with the SNHG family score, suggesting that a more complex interplay between DNA damage repair and immunity deserves further research.

SNHGs play adverse functional roles in LUAD,[50,51] which is consistent with our findings and supports our results. The differential genes between high and low SNHG family scores in LUAD were used to establish a prognostic risk model by LASSO–Cox regression analysis. The KM survival analysis and ROC of the TCGA–LUAD cohort and GEO validation cohorts indicated that the risk score had good survival predictive ability. Meanwhile, the same analyses generalized the risk score to pan-cancer. Functional analysis showed that the risk score was positively related to the status of hypoxia, same with the SNHG family score, and may be the reason for the higher activity of the P53 pathway in the high-risk group.[44] Glycolysis, the key biochemical fingerprint of altered energy metabolism in cancers, not only conferred a selective advantage on cancer cells under a diminished nutrient supply; in addition, it provided metabolic intermediates for macromolecular biosynthesis and the formation of an immunosuppressive microenvironment.[39,52] Thus, the relation between risk score and glycolysis activity further explained the higher degree of malignancy of the high-risk group, compared with the low-risk group.

These changes in functions and pathways shaped the immunosuppressive microenvironment characterized by low immune cells ($CD8^+$ T/T cells, B cells, monocytes, and neutrophils) and high cancer-promoting fibroblasts in high-risk patients. Thus, we hypothesized that the risk score can be a predictor of immunotherapy. With respect to TIDE and IPS, patients in the low-risk group were more sensitive to immunotherapy. In addition, 4 immunotherapy cohorts (IMvigor210, GSE78220, GSE91061, and GSE126044) verified the conclusion. Meanwhile,

drug sensitivity analysis showed that chemotherapy drugs were more suitable for high-risk patients than for the high-risk and low-risk groups. Overall, these results suggest that the SNHG-related risk score could be a potential biomarker for immunotherapy response.

In conclusion, our comprehensive pan-cancer analysis of the SNHG family illustrates the landscape of SNHGs in multiple cancer types. The SNHG family score and a novel 12-gene signature were established for pan-cancer on the basis of the expression. Our data suggest that the SNHG family score and risk score can serve as biomarkers for the prognosis of most cancers. Further functional analysis indicated that biomarkers were significantly related to the hypoxic phenotype of the TME. Meanwhile, biomarkers shaped the immunosuppressive microenvironment mainly mediated by $CD8^+$ T cells, M2 macrophages, and cancer-promoting fibroblasts. We further found that the SNHG-related risk score can be a potential biomarker for CIT response in multiple cancers. In this study, we comprehensively analyze the SNHGs in pan-cancer, explore the effect of SNHGs on tumor development and immunity, and potentially provide more accurate CIT for patients in the future.

Limitations of the study

The present study has several potential limitations. First, the association between SNHGs and the immunotherapy response was identified by public data and lacks clinical validation. Second, this study lacks relevant verification at the molecular level, which will be verified in subsequent studies.

STAR★METHODS

Detailed methods are provided in the online version of this paper and include the following:

- KEY RESOURCES TABLE
- RESOURCE AVAILABILITY
  - Lead contact
  - Materials availability
  - Data and code availability
- EXPERIMENTAL MODEL AND STUDY PARTICIPANT DETAILS
  - Data collection and preparation
- METHOD DETAILS
  - Expression, mutation, and drug sensitivity analyses of SNHGs
  - Evaluation and calculation of SNHG family score
  - Functional and immune environment analyses of SNHG family score
  - Relationships between SNHG family score and immunotherapy indicators
  - Construction and validation of SNHG-related prognostic risk model
  - Functional, pathway, and immune analyses of SNHG-related risk score
  - Predictive value of SNHG-related risk score in immunotherapy and chemotherapy
- QUANTIFICATION AND STATISTICAL ANALYSIS

SUPPLEMENTAL INFORMATION

Supplemental information can be found online at https://doi.org/10.1016/j.isci.2023.108055.

ACKNOWLEDGMENTS

This study was supported by Shandong Provincial Natural Science Foundation [Grant number ZR2021MH192 and ZR2020QH215]. We are grateful to all public databases involved in this study. We thank Shanghai Tengyun Biotechnology Co., Ltd. for developing the Hiplot Pro platform (https://hiplot.com.cn/) and providing technical assistance and valuable tools for conducting data analysis and visualization.

AUTHOR CONTRIBUTIONS

All authors contributed to the study conception and design. H.Z., G.W., and J.D. carried out the design of the study, the analyses of the statistics, the creation of new software used in the work and the drafting of the manuscript. H.Z., G.W., Y.W., and J.L. carried out the collection of the statistics and the preparation of the manuscript. All the authors read and approved the final manuscript.

DECLARATION OF INTERESTS

The authors declare no competing interests.

Received: April 24, 2023
Revised: August 16, 2023
Accepted: September 22, 2023
Published: September 25, 2023

REFERENCES

1. He, X., and Xu, C. (2020). Immune checkpoint signaling and cancer immunotherapy. Cell Res. *30*, 660–669. https://doi.org/10.1038/s41422-020-0343-4.
2. Hegde, P.S., and Chen, D.S. (2020). Top 10 Challenges in Cancer Immunotherapy. Immunity *52*, 17–35. https://doi.org/10.1016/j.immuni.2019.12.011.
3. Topalian, S.L., Taube, J.M., Anders, R.A., and Pardoll, D.M. (2016). Mechanism-driven biomarkers to guide immune checkpoint blockade in cancer therapy. Nat. Rev. Cancer *16*, 275–287. https://doi.org/10.1038/nrc.2016.36.
4. Topalian, S.L., Sznol, M., McDermott, D.F., Kluger, H.M., Carvajal, R.D., Sharfman, W.H., Brahmer, J.R., Lawrence, D.P., Atkins, M.B., Powderly, J.D., et al. (2014). Survival, durable tumor remission, and long-term safety in patients with advanced melanoma receiving nivolumab. J. Clin. Oncol. *32*, 1020–1030. https://doi.org/10.1200/JCO.2013.53.0105.
5. Hamid, O., Robert, C., Daud, A., Hodi, F.S., Hwu, W.J., Kefford, R., Wolchok, J.D., Hersey, P., Joseph, R.W., Weber, J.S., et al. (2013). Safety and tumor responses with lambrolizumab (anti-PD-1) in melanoma. N. Engl. J. Med. *369*, 134–144. https://doi.org/10.1056/NEJMoa1305133.
6. Robert, C., Schachter, J., Long, G.V., Arance, A., Grob, J.J., Mortier, L., Daud, A., Carlino, M.S., McNeil, C., Lotem, M., et al. (2015). Pembrolizumab versus Ipilimumab in Advanced Melanoma. N. Engl. J. Med. *372*, 2521–2532. https://doi.org/10.1056/NEJMoa1503093.
7. Robert, C., Long, G.V., Brady, B., Dutriaux, C., Maio, M., Mortier, L., Hassel, J.C., Rutkowski, P., McNeil, C., Kalinka-Warzocha, E., et al. (2015). Nivolumab in previously untreated melanoma without BRAF mutation. N. Engl. J. Med. *372*, 320–330. https://doi.org/10.1056/NEJMoa1412082.
8. Larkin, J., Chiarion-Sileni, V., Gonzalez, R., Grob, J.J., Cowey, C.L., Lao, C.D., Schadendorf, D., Dummer, R., Smylie, M., Rutkowski, P., et al. (2015). Combined Nivolumab and Ipilimumab or Monotherapy in Untreated Melanoma. N. Engl. J. Med. *373*, 23–34. https://doi.org/10.1056/NEJMoa1504030.
9. Borghaei, H., Paz-Ares, L., Horn, L., Spigel, D.R., Steins, M., Ready, N.E., Chow, L.Q., Vokes, E.E., Felip, E., Holgado, E., et al. (2015). Nivolumab versus Docetaxel in Advanced Nonsquamous Non-Small-Cell Lung Cancer. N. Engl. J. Med. *373*, 1627–1639. https://doi.org/10.1056/NEJMoa1507643.
10. Brahmer, J., Reckamp, K.L., Baas, P., Crinò, L., Eberhardt, W.E.E., Poddubskaya, E., Antonia, S., Pluzanski, A., Vokes, E.E., Holgado, E., et al. (2015). Nivolumab versus Docetaxel in Advanced Squamous-Cell Non-Small-Cell Lung Cancer. N. Engl. J. Med. *373*, 123–135. https://doi.org/10.1056/NEJMoa1504627.
11. Garon, E.B., Rizvi, N.A., Hui, R., Leighl, N., Balmanoukian, A.S., Eder, J.P., Patnaik, A., Aggarwal, C., Gubens, M., Horn, L., et al. (2015). Pembrolizumab for the treatment of non-small-cell lung cancer. N. Engl. J. Med. *372*, 2018–2028. https://doi.org/10.1056/NEJMoa1501824.
12. Motzer, R.J., Escudier, B., McDermott, D.F., George, S., Hammers, H.J., Srinivas, S., Tykodi, S.S., Sosman, J.A., Procopio, G., Plimack, E.R., et al. (2015). Nivolumab versus Everolimus in Advanced Renal-Cell Carcinoma. N. Engl. J. Med. *373*, 1803–1813. https://doi.org/10.1056/NEJMoa1510665.
13. Motzer, R.J., Rini, B.I., McDermott, D.F., Redman, B.G., Kuzel, T.M., Harrison, M.R., Vaishampayan, U.N., Drabkin, H.A., George, S., Logan, T.F., et al. (2015). Nivolumab for Metastatic Renal Cell Carcinoma: Results of a Randomized Phase II Trial. J. Clin. Oncol. *33*, 1430–1437. https://doi.org/10.1200/JCO.2014.59.0703.
14. Topalian, S.L., Hodi, F.S., Brahmer, J.R., Gettinger, S.N., Smith, D.C., McDermott, D.F., Powderly, J.D., Carvajal, R.D., Sosman, J.A., Atkins, M.B., et al. (2012). Safety, activity, and immune correlates of anti-PD-1 antibody in cancer. N. Engl. J. Med. *366*, 2443–2454. https://doi.org/10.1056/NEJMoa1200690.
15. Sharma, P., Hu-Lieskovan, S., Wargo, J.A., and Ribas, A. (2017). Primary, Adaptive, and Acquired Resistance to Cancer Immunotherapy. Cell *168*, 707–723. https://doi.org/10.1016/j.cell.2017.01.017.
16. Goodall, G.J., and Wickramasinghe, V.O. (2021). RNA in cancer. Nat. Rev. Cancer *21*, 22–36. https://doi.org/10.1038/s41568-020-00306-0.
17. Atianand, M.K., Caffrey, D.R., and Fitzgerald, K.A. (2017). Immunobiology of Long Noncoding RNAs. Annu. Rev. Immunol. *35*, 177–198. https://doi.org/10.1146/annurev-immunol-041015-055459.
18. Zhou, Y., Sun, W., Qin, Z., Guo, S., Kang, Y., Zeng, S., and Yu, L. (2021). LncRNA regulation: New frontiers in epigenetic solutions to drug chemoresistance. Biochem. Pharmacol. *189*, 114228. https://doi.org/10.1016/j.bcp.2020.114228.
19. Tan, Y.T., Lin, J.F., Li, T., Li, J.J., Xu, R.H., and Ju, H.Q. (2021). LncRNA-mediated posttranslational modifications and reprogramming of energy metabolism in cancer. Cancer Commun. *41*, 109–120. https://doi.org/10.1002/cac2.12108.
20. Zhang, M., Wang, N., Song, P., Fu, Y., Ren, Y., Li, Z., and Wang, J. (2020). LncRNA GATA3-AS1 facilitates tumour progression and immune escape in triple-negative breast cancer through destabilization of GATA3 but stabilization of PD-L1. Cell Prolif. *53*, e12855. https://doi.org/10.1111/cpr.12855.
21. Xu, H., Jiang, Y., Xu, X., Su, X., Liu, Y., Ma, Y., Zhao, Y., Shen, Z., Huang, B., and Cao, X. (2019). Inducible degradation of lncRNA Sros1 promotes IFN-gamma-mediated activation of innate immune responses by stabilizing Stat1 mRNA. Nat. Immunol. *20*, 1621–1630. https://doi.org/10.1038/s41590-019-0542-7.
22. Li, G., Kryczek, I., Nam, J., Li, X., Li, S., Li, J., Wei, S., Grove, S., Vatan, L., Zhou, J., et al. (2021). LIMIT is an immunogenic lncRNA in cancer immunity and immunotherapy. Nat. Cell Biol. *23*, 526–537. https://doi.org/10.1038/s41556-021-00672-3.
23. Krawczyk, M., and Emerson, B.M. (2014). p50-associated COX-2 extragenic RNA (PACER) activates COX-2 gene expression by occluding repressive NF-kappaB complexes. Elife *3*, e01776. https://doi.org/10.7554/eLife.01776.
24. Zhou, Y., Zhu, Y., Xie, Y., and Ma, X. (2019). The Role of Long Non-coding RNAs in Immunotherapy Resistance. Front. Oncol. *9*, 1292. https://doi.org/10.3389/fonc.2019.01292.
25. Egranov, S.D., Hu, Q., Lin, C., and Yang, L. (2020). LncRNAs as tumor cell intrinsic factors that affect cancer immunotherapy. RNA Biol. *17*, 1625–1627. https://doi.org/10.1080/15476286.2020.1767455.
26. Jiang, W., Pan, S., Chen, X., Wang, Z.W., and Zhu, X. (2021). The role of lncRNAs and circRNAs in the PD-1/PD-L1 pathway in cancer immunotherapy. Mol. Cancer *20*, 116. https://doi.org/10.1186/s12943-021-01406-7.
27. Zimta, A.A., Tigu, A.B., Braicu, C., Stefan, C., Ionescu, C., and Berindan-Neagoe, I. (2020). An Emerging Class of Long Non-coding RNA With Oncogenic Role Arises From the snoRNA Host Genes. Front. Oncol. *10*, 389. https://doi.org/10.3389/fonc.2020.00389.
28. Yang, H., Jiang, Z., Wang, S., Zhao, Y., Song, X., Xiao, Y., and Yang, S. (2019). Long non-coding small nucleolar RNA host genes in digestive cancers. Cancer Med. *8*, 7693–7704. https://doi.org/10.1002/cam4.2622.
29. Kufel, J., and Grzechnik, P. (2019). Small Nucleolar RNAs Tell a Different Tale. Trends Genet. *35*, 104–117. https://doi.org/10.1016/j.tig.2018.11.005.
30. Romano, G., Veneziano, D., Acunzo, M., and Croce, C.M. (2017). Small non-coding RNA and cancer. Carcinogenesis *38*, 485–491. https://doi.org/10.1093/carcin/bgx026.
31. Huang, Y., Xia, L., Tan, X., Zhang, J., Zeng, W., Tan, B., Yu, X., Fang, W., and Yang, Z. (2022). Molecular mechanism of lncRNA SNHG12 in immune escape of non-small cell lung cancer through the HuR/PD-L1/USP8 axis. Cell. Mol. Biol. Lett. *27*, 43. https://doi.org/10.1186/s11658-022-00343-7.
32. Pei, X., Wang, X., and Li, H. (2018). LncRNA SNHG1 regulates the differentiation of Treg cells and affects the immune escape of breast cancer via regulating miR-448/IDO. Int. J. Biol. Macromol. *118*, 24–30. https://doi.org/10.1016/j.ijbiomac.2018.06.033.
33. Zhang, Y., Li, B., Bai, Q., Wang, P., Wei, G., Li, Z., Hu, L., Tian, Q., Zhou, J., Huang, Q., et al. (2021). The lncRNA Snhg1-Vps13D vesicle trafficking system promotes memory CD8 T cell establishment via regulating the dual effects of IL-7 signaling. Signal Transduct. Targeted Ther. *6*, 126. https://doi.org/10.1038/s41392-021-00492-9.
34. Qian, M., Ling, W., and Ruan, Z. (2020). Long non-coding RNA SNHG12 promotes immune escape of ovarian cancer cells through their crosstalk with M2 macrophages. Aging (Albany NY) *12*, 17122. https://doi.org/10.18632/aging.103653.
35. Denton, A.E., Roberts, E.W., and Fearon, D.T. (2018). Stromal Cells in the Tumor Microenvironment. Adv. Exp. Med. Biol. *1060*, 99–114. https://doi.org/10.1007/978-3-319-78127-3_6.
36. Qian, J., Olbrecht, S., Boeckx, B., Vos, H., Laoui, D., Etlioglu, E., Wauters, E., Pomella, V., Verbandt, S., Busschaert, P., et al. (2020). A pan-cancer blueprint of the heterogeneous tumor microenvironment revealed by single-cell profiling. Cell Res. *30*, 745–762. https://doi.org/10.1038/s41422-020-0355-0.
37. Wu, Z., Zuo, M., Zeng, L., Cui, K., Liu, B., Yan, C., Chen, L., Dong, J., Shangguan, F., Hu, W., et al. (2021). OMA1 reprograms metabolism under hypoxia to promote colorectal cancer development. EMBO Rep. *22*, e50827. https://doi.org/10.15252/embr.202050827.
38. Peng, F., Wang, J.H., Fan, W.J., Meng, Y.T., Li, M.M., Li, T.T., Cui, B., Wang, H.F., Zhao, Y., An, F., et al. (2018). Glycolysis gatekeeper

PDK1 reprograms breast cancer stem cells under hypoxia. Oncogene *37*, 1062–1074. https://doi.org/10.1038/onc.2017.368.

39. Morrissey, S.M., Zhang, F., Ding, C., Montoya-Durango, D.E., Hu, X., Yang, C., Wang, Z., Yuan, F., Fox, M., Zhang, H.G., et al. (2021). Tumor-derived exosomes drive immunosuppressive macrophages in a pre-metastatic niche through glycolytic dominant metabolic reprogramming. Cell Metabol. *33*, 2040–2058.e10. https://doi.org/10.1016/j.cmet.2021.09.002.
40. Gao, J., Zeng, K., Liu, Y., Gao, L., and Liu, L. (2019). LncRNA SNHG5 promotes growth and invasion in melanoma by regulating the miR-26a-5p/TRPC3 pathway. OncoTargets Ther. *12*, 169–179. https://doi.org/10.2147/OTT.S184078.
41. Wei, S., Sun, S., Zhou, X., Zhang, C., Li, X., Dai, S., Wang, Y., Zhao, L., and Shan, B. (2021). SNHG5 inhibits the progression of EMT through the ubiquitin-degradation of MTA2 in oesophageal cancer. Carcinogenesis *42*, 315–326. https://doi.org/10.1093/carcin/bgaa110.
42. Sanchez-Vega, F., Mina, M., Armenia, J., Chatila, W.K., Luna, A., La, K.C., Dimitriadoy, S., Liu, D.L., Kantheti, H.S., Saghafinia, S., et al. (2018). Oncogenic Signaling Pathways in The Cancer Genome Atlas. Cell *173*, 321–337.e10.e310. https://doi.org/10.1016/j.cell.2018.03.035.
43. Viallard, C., and Larrivée, B. (2017). Tumor angiogenesis and vascular normalization: alternative therapeutic targets. Angiogenesis *20*, 409–426. https://doi.org/10.1007/s10456-017-9562-9.
44. Jing, X., Yang, F., Shao, C., Wei, K., Xie, M., Shen, H., and Shu, Y. (2019). Role of hypoxia in cancer therapy by regulating the tumor microenvironment. Mol. Cancer *18*, 157. https://doi.org/10.1186/s12943-019-1089-9.
45. Diakos, C.I., Charles, K.A., McMillan, D.C., and Clarke, S.J. (2014). Cancer-related inflammation and treatment effectiveness. Lancet Oncol. *15*, e493–e503. https://doi.org/10.1016/s1470-2045(14)70263-3.
46. Fan, Y., Gao, Z., Xu, J., Wang, H., Guo, Q., Xue, H., Zhao, R., Guo, X., and Li, G. (2022). Identification and validation of SNHG gene signature to predict malignant behaviors and therapeutic responses in glioblastoma. Front. Immunol. *13*, 986615. https://doi.org/10.3389/fimmu.2022.986615.
47. Cheng, H., Wang, Z., Fu, L., and Xu, T. (2019). Macrophage Polarization in the Development and Progression of Ovarian Cancers: An Overview. Front. Oncol. *9*, 421. https://doi.org/10.3389/fonc.2019.00421.
48. Mills, C.D. (2015). Anatomy of a discovery: m1 and m2 macrophages. Front. Immunol. *6*, 212. https://doi.org/10.3389/fimmu.2015.00212.
49. Mills, C.D., Kincaid, K., Alt, J.M., Heilman, M.J., and Hill, A.M. (2000). M-1/M-2 macrophages and the Th1/Th2 paradigm. J. Immunol. *164*, 6166–6173. https://doi.org/10.4049/jimmunol.164.12.6166.
50. Pei, Y.F., He, Y., Hu, L.Z., Zhou, B., Xu, H.Y., and Liu, X.Q. (2020). The Crosstalk between lncRNA-SNHG7/miRNA-181/cbx7 Modulates Malignant Character in Lung Adenocarcinoma. Am. J. Pathol. *190*, 1343–1354. https://doi.org/10.1016/j.ajpath.2020.02.011.
51. Li, W., Zheng, Y., Mao, B., Wang, F., Zhong, Y., and Cheng, D. (2020). SNHG17 upregulates WLS expression to accelerate lung adenocarcinoma progression by sponging miR-485-5p. Biochem. Biophys. Res. Commun. *533*, 1435–1441. https://doi.org/10.1016/j.bbrc.2020.09.130.
52. Ganapathy-Kanniappan, S., and Geschwind, J.-F.H. (2013). Tumor Glycolysis as a Target for Cancer Therapy: Progress and Prospects (Molecular Cancer).
53. Hanzelmann, S., Castelo, R., and Guinney, J. (2013). GSVA: gene set variation analysis for microarray and RNA-seq data. BMC Bioinf. *14*, 1–15.
54. Yuan, H., Yan, M., Zhang, G., Liu, W., Deng, C., Liao, G., Xu, L., Luo, T., Yan, H., Long, Z., et al. (2019). CancerSEA: a cancer single-cell state atlas. Nucleic Acids Res. *47*, D900–D908. https://doi.org/10.1093/nar/gky939.
55. Newman, A.M., Liu, C.L., Green, M.R., Gentles, A.J., Feng, W., Xu, Y., Hoang, C.D., Diehn, M., and Alizadeh, A.A. (2015). Robust enumeration of cell subsets from tissue expression profiles. Nat. Methods *12*, 453–457. https://doi.org/10.1038/nmeth.3337.
56. Yarchoan, M., Hopkins, A., and Jaffee, E.M. (2017). Tumor Mutational Burden and Response Rate to PD-1 Inhibition. N. Engl. J. Med. *377*, 2500–2501. https://doi.org/10.1056/NEJMc1713444.
57. Le, D.T., Uram, J.N., Wang, H., Bartlett, B.R., Kemberling, H., Eyring, A.D., Skora, A.D., Luber, B.S., Azad, N.S., Laheru, D., et al. (2015). PD-1 Blockade in Tumors with Mismatch-Repair Deficiency. N. Engl. J. Med. *372*, 2509–2520. https://doi.org/10.1056/NEJMoa1500596.
58. Jiang, P., Gu, S., Pan, D., Fu, J., Sahu, A., Hu, X., Li, Z., Traugh, N., Bu, X., Li, B., et al. (2018). Signatures of T cell dysfunction and exclusion predict cancer immunotherapy response. Nat. Med. *24*, 1550–1558. https://doi.org/10.1038/s41591-018-0136-1.
59. Rooney, M.S., Shukla, S.A., Wu, C.J., Getz, G., and Hacohen, N. (2015). Molecular and genetic properties of tumors associated with local immune cytolytic activity. Cell *160*, 48–61. https://doi.org/10.1016/j.cell.2014.12.033.
60. Yoshihara, K., Shahmoradgoli, M., Martínez, E., Vegesna, R., Kim, H., Torres-Garcia, W., Treviño, V., Shen, H., Laird, P.W., Levine, D.A., et al. (2013). Inferring tumour purity and stromal and immune cell admixture from expression data. Nat. Commun. *4*, 2612. https://doi.org/10.1038/ncomms3612.
61. Becht, E., Giraldo, N.A., Lacroix, L., Buttard, B., Elarouci, N., Petitprez, F., Selves, J., Laurent-Puig, P., Sautès-Fridman, C., Fridman, W.H., and de Reyniès, A. (2016). Estimating the population abundance of tissue-infiltrating immune and stromal cell populations using gene expression. Genome Biol. *17*, 218. https://doi.org/10.1186/s13059-016-1070-5.
62. Charoentong, P., Finotello, F., Angelova, M., Mayer, C., Efremova, M., Rieder, D., Hackl, H., and Trajanoski, Z. (2017). Pan-cancer Immunogenomic Analyses Reveal Genotype-Immunophenotype Relationships and Predictors of Response to Checkpoint Blockade. Cell Rep. *18*, 248–262. https://doi.org/10.1016/j.celrep.2016.12.019.
63. Geeleher, P., Cox, N., and Huang, R.S. (2014). pRRophetic: an R package for prediction of clinical chemotherapeutic response from tumor gene expression levels. PLoS One *9*, e107468. https://doi.org/10.1371/journal.pone.0107468.

STAR★METHODS

KEY RESOURCES TABLE

REAGENT or RESOURCE	SOURCE	IDENTIFIER
Software and algorithms		
R	R software	https://www.r-project.org/
GraphPad Prism 8	GraphPad software	https://www.graphpad.com/

RESOURCE AVAILABILITY

Lead contact

Further information and requests for resources should be directed to the lead contact, Jiajun Du (dujiajun@sdu.edu.cn).

Materials availability

This study did not generate any new unique materials.

Data and code availability

- Deidentified final results supporting this study are available for research purposes upon reasonable written request to the corresponding author.
- No unique code was generated during the study. But code supporting this study are available from the corresponding author.
- Any additional information required to reanalyze the data reported in this paper is available from the lead contact upon request.

EXPERIMENTAL MODEL AND STUDY PARTICIPANT DETAILS

Data collection and preparation

Gene expression data and associated clinical data for 33 cancer types and normal tissues were downloaded from the TCGA data portal (https://portal.gdc.cancer.gov/), UCSC Xena (https://xena.ucsc.edu/) and GTEx (https://gtexportal.org/home/) databases. Data on gene somatic mutations were also downloaded from the TCGA database. The GEO https://www.ncbi.nlm.nih.gov/geo/) database provided the lung adenocarcinoma (LUAD) cohorts, including expression data and clinical data (GSE3141, GSE31210, GSE30219, GSE37745). The immunotherapy response datasets employed were from the GEO database (GSE78220, GSE91061, GSE126044). The IMvigor210 cohort, which consisted of patients with metastatic urothelial cancer treated using an anti-PD-L1 agent (atezolizumab), was available under the Creative Commons 3.0 license and can be downloaded from http://research-pub.gene.com/IMvigor210CoreBiologies.

METHOD DETAILS

Expression, mutation, and drug sensitivity analyses of SNHGs

To evaluate the significance of SNHGs, we extracted and revealed the expression of 31 SNHGs (Table S1) in pan-cancer from the TCGA database. Differential expression analysis for SNHGs was performed based on the limma package in R. Depending on the MAF files from the TCGA database, somatic mutation analysis for each cancer type was performed to identify the status of the single-nucleotide variant (SNV) of SNHGs by using the maftools package in R. DNA methylation, copy number variations (CNVs), and drug sensitivity analyses of SNHGs were explored using the GSCA database (http://bioinfo.life.hust.edu.cn/GSCA/#/). However, not all SNHGs were explored in the pan-cancer analysis.

Evaluation and calculation of SNHG family score

The SNHG family score was calculated based on single-sample gene set enrichment analysis (ssGSEA)[53] by using the SNHG set to quantify the expression levels of these genes for each cancer. We estimated the SNHG family score between tumor and normal samples in 33 cancers from the TCGA and GTEx datasets. In 3 (CHOL, MESO, and UVM) of the 33 cancers, the score was calculated for the tumor samples only as the normal samples were not inadequate. In other cancers, differential analysis was performed. Tumor tissues were divided into the high-score and low-score groups, depending on the optimal cutoffs for OS in pan-cancer. The survival curves of the SNHG family scores in different tumors were plotted by R software.

Functional and immune environment analyses of SNHG family score

The database CancerSEA (http://biocc.hrbmu.edu.cn/CancerSEA/) was used to evaluate the correlation between the SNHG family score and the diverse functional states of cancer at a single-cell resolution.[54] Immune score and stroma score from xCell (https://xcell.ucsf.edu/) were

used to reflect the composition of the TME in pan-cancer. More detailed immune cell infiltration was extracted from TIMER (http://timer.cistrome.org/) based on the CIBERSORT algorithm to evaluate the immune status of pan-cancer.[55] As key factors in the immune environment, immune checkpoints, immune-activating and -suppressing genes, and chemokine and chemokine receptor genes, are listed in Table S2. The correlation analyses between the SNHG family score and these aforementioned indicators of immune status were used to show the role of the score in the immune environment.

Relationships between SNHG family score and immunotherapy indicators

TMB is typically measured by the number of somatic mutations in the coding region of the tumor cell genome. TMB has been identified as a quantifiable biomarker for evaluating the therapeutic effect of CIT.[56] Microsatellite instability (MSI) is used to reflect the functional deficiency in the repair of DNA mismatches in tumor tissues; meanwhile, the deficiency has been confirmed to be a marker of the PD-1 antibody.[57] On the basis of the TCGA and UCSC Xena data, the TMB and MSI values were acquired to analyze their relationship with the SNHG family score. Tumor immune dysfunction and exclusion (TIDE) was developed as a computational method to identify signatures of both T cell dysfunction and exclusion, efficiently predicting the tumor immune evasion status and the response and resistance to checkpoint blockade.[58] Data on 22 cancers provided by the TIDE database were used to analyze the correlation TIDE with the SNHG family score (http://tide.dfci.harvard.edu/).

Construction and validation of SNHG-related prognostic risk model

Differential expression analysis was conducted on the groups with high and low SNHG family scores in LUAD (340 vs. 155 samples) by using the limma package, with different screening parameters (|logFC| > 1, FDR (false discovery rate) < 0.05). Differentially expressed genes with prognostic values were further screened out by univariate Cox regression analysis. LASSO-Cox regression analysis was used to construct an SNHG-related prognostic risk model and obtain a risk gene signature. The risk score was formulated as follows:

$$\text{Risk Score} = \sum_{i=1}^{n} Coef(i) * Exp(i)$$

where n is the number of genes in the model, Exp (i) is the expression level of the genes, and Coef (i) is the estimated regression coefficient of the genes in the regression model. Meanwhile, the same genes were used to estimate the risk score of the validation cohorts. The median risk score was used as a cutoff to divide the patients in the training and validation cohorts into two groups: the low-risk and high-risk groups.

Kaplan–Meier (KM) survival curves, time-dependent receiver operating characteristic (ROC) curves, and the area under the curve (AUC) were estimated to evaluate the sensitivity and specificity of the risk score. Univariate and multivariate Cox regression analyses were performed to identify independent prognostic factors. The relationship between clinicopathological characteristics and risk score was determined by correlation analysis. Risk factor analysis was used to show the correlation between risk score and survival status. The same analyses were conducted on four independent validation cohorts to strengthen the reliability of the conclusions. Meanwhile, we generalized the risk score by using the same method that applied in pan-cancer analysis to evaluate the fitness of the model.

Functional, pathway, and immune analyses of SNHG-related risk score

Gene set variation analysis,[53] which estimates variations in pathway activity, was employed to analyze differences in the immune function, signaling pathways, and hallmarks of cancers between two risk groups from the GSEA database (http://www.gsea-msigdb.org/gsea/login.jsp) and Rooney, M. S. et al.[59] The correlation between immune checkpoints and risk score was also analyzed. The stromal, immune, and ESTIMATE scores were calculated using the ESTIMATE algorithm[60] to examine the effect of risk score on TME, based on the transcriptome expression profiles of LUAD. Microenvironment Cell Populations-counter (MCP-counter) analysis, which allowed the robust quantification of the absolute abundance of 8 immune and 2 stromal cell populations, further refined the composition of the TME.[61]

Predictive value of SNHG-related risk score in immunotherapy and chemotherapy

Immunotherapy responsiveness in high- and low-risk groups was evaluated using TIDE and immunophenoscore (IPS)[62] for LUAD and pan-cancer, respectively. Survival analysis, differences in immunotherapy response rates, and ROCs of immunotherapy cohorts (IMvigor210, GSE78220, GSE91061, and GSE126044) were used to assess the predictive value of the risk score. We performed a drug sensitivity analysis using the pRRophetic package to evaluate the relationship between chemotherapeutic response and risk score.[63]

QUANTIFICATION AND STATISTICAL ANALYSIS

Survival analysis was conducted using the KM method, and correlation analyses were analyzed by Spearman correlation analysis. Visualization of the aforementioned was performed in R version 4.0.2 (http://www.r-project.org/). A two-tailed P-value <0.05 was considered statistically significant. *p < 0.05; **p < 0.01 and ***p < 0.001, ****p < 0.0001; ns, not significant.